Time-domain numerical analysis of single pedestrian random walks on laminated glass slabs in pre- or post-breakage regime

Chiara Bedon

University of Trieste, Department of Engineering and Architecture, 34127 Trieste, Italy

ARTICLE INFO

Keywords:
Walking paths
Laminated glass (LG) slab
Post-breakage vibration
On-site experiments
Finite Element (FE) numerical modelling

ABSTRACT

Mechanical performance assessment of load-bearing elements under ordinary design actions is a priority when material degradation or even severe damage may be experienced. This is especially the case of unconventional constructional materials, or assembled systems like laminated glass (LG) solutions, in which multiple load-bearing components may suffer of different mechanical issues. This turns out in potential risk for customers, and in the need of specific design assumptions to address the problem. For load-bearing elements with direct interaction with final users (as pedestrian systems), a reciprocal modification of mechanical and dynamic parameters should be properly taken into account in the early design process.

This paper explores the sensitivity of human-structure interaction effects and performance indicators for LG slab modules subjected to various walking paths of single pedestrians. An extended set of Finite Element (FE) nonlinear dynamic numerical simulations is presented, in which the variation of conventional performance indicators (such as acceleration peaks, deflection, vibration frequency) is investigated for two in-service LG modular units with intact (LGU) or partially fractured (LGF) glass layers. Walking scenarios are described with the support of consolidated deterministic method in use for pedestrian loads, in which walking features do not account for the features of structural background. The comparative analysis of numerical results with earlier experimental outcomes for two reference LG slab modules subjected to random walking conditions shows that time-domain nonlinear simulations with simplified pedestrian loads can efficiently capture some major effects of pedestrians, as well as the presence of damage in glass. At the same time, it is shown that fractured glass layers in LG pedestrian modules can still provide partial post-breakage contribution to the resisting section.

1. Introduction

Given the increasingly use of laminated glass (LG) components in buildings, knowledge and appropriate description of post-breakage residual stiffness and residual strength is of utmost importance for design considerations [1–3]. Due to intrinsic material brittleness, the analysis of possible damage scenarios and assessment of fractured LG elements is a crucial issue [4].

Besides, the post-breakage performance of LG elements is a rather complex phenomenon, which is characterized by the presence of glass fragments that are expected to adhere to the residual section (thanks to bonding interlayers) and provide some stiffness and mass contribution to the original composite layout.

Multiple aspects are implicitly involved in the definition of key mechanical parameters that govern the uncertain post-breakage response of LG members, like fragmentation of glass, fragment size, interlayer type, ambient conditions, strain rate, etc. [5], and few literature studies can be found to support the in-depth analysis of structural glass members under specific laboratory conditions. Examples can in fact be found for deliberately pre-cracked LG panels [6,7], LG balustrades with cracked layers [8], fractured columns under impact [9], beams and connections in samples affected by partial glass fracture [10–12], and others [13–15]. In this direction, various analytical models and computationally refined Finite Element (FE) numerical tools have been also elaborated. Among others, a simplified analytical approach has been presented in [16,17] for fully cracked LG elements under tensile loads, in order to predict the bridge effect of interlayers. Preliminary numerical models based on Cohesive Zone Modelling (CZM) technique have been presented in [18] for small-scale fractured samples under high temperature and in-plane bending. Impact simulations have been presented in [19] to critically assess the post-breakage performance capacity of LG panels under blast. In [20], the pre- and post-breakage analysis for LG in out-of-plane bending has been explored. Experimental data from quasit-static setup were used for the validation

E-mail address: chiara.bedon@dia.units.it.

of a refined phase-field based numerical model inclusive of glass fracture and viscoelasticity for the interlayer. A micro–macro approach inclusive of homogenization and elementary cell concepts with CZM has been presented in [21] for the study of in-plane loaded small fragments of tempered glass (Fig. 1(a)). It was shown that the stress pattern of a single fragment can be efficiently described and homogenised to describe the response of a given element, but major uncertainty relies on the actual bonding (or possible debonding) of fragments from interlayers.

The numerical investigation reported in [8] introduced, with the support of full-scale experimental validations from the impact response of balustrades in out-of-plane bending, the simplified concept of calibrated equivalent modulus (MoE) to efficiently describe the residual capacity of fractured tempered glass layers for LG members in out-of-plane bending (Fig. 1(b)). Such a mechanically simplified concept assumes that the LG bending response is mainly governed by a fractured glass layer which can contribute in compression or tensile region respectively. Consequently, glass fragments are assumed kept together by interlayers and intact glass panes, and homogenised by a reduced MoE (Section 2). This kind of elaboration follows the existing design assumptions for glass [1–3], where conventional calculations at the Collapse Limit State are based on the physical removal of a sacrificial / fractured glass layer from the LG section to verify (Fig. 1(c), with fragments on the tension side). While safe, such a kind of approach fully disregards any king of collaboration of glass fragments from the resting cross-section with damage [8]. The result is that severely conservative assumptions are often taken into account for FE numerical purposes, or rather complex experimental / numerical protocols should be followed quantify the actual damage sensitivity and residual capacity of fractured LGs. Moreover, the approach does not account for other possible accidental damage scenarios as in Fig. 1(c), where fragments on the compression side (for the examined loading setup) are expected to offer improved residual capacity compared to tension side. Finally, the cyclical bending regime which affects the residual LG section (with fragments still in place) under pedestrian motion should be also addressed.

In this paper, a still open issue is investigated for LG in buildings. A special attention is given to the FE numerical analysis of pedestrian LG modules which are expected to sustain ordinary walking paths and vibrate in out-of-plane bending (due to customers), but could also to suffer for partial degradation in operational time, such as possible fracture of glass layers for in-service structural systems subjected to accidental scenarios under normal use. While it is known that vibrations of glass members can be generally sensitive to boundaries, occupancy levels and walking features [22–25], limited literature efforts are still available to judge the potential of FE numerical tools to efficiently predict the expected critical scenarios, and thus optimize the structural analysis of such a kind of vulnerable building components.

2. Research methodology

2.1. Goals

The present research investigation arises from the current need of more in-depth discussion and knowledge about the actual post-breakage and vibration performance of LG members in buildings, as well as from the detection of a reference in-service LG walkway suffering from partial

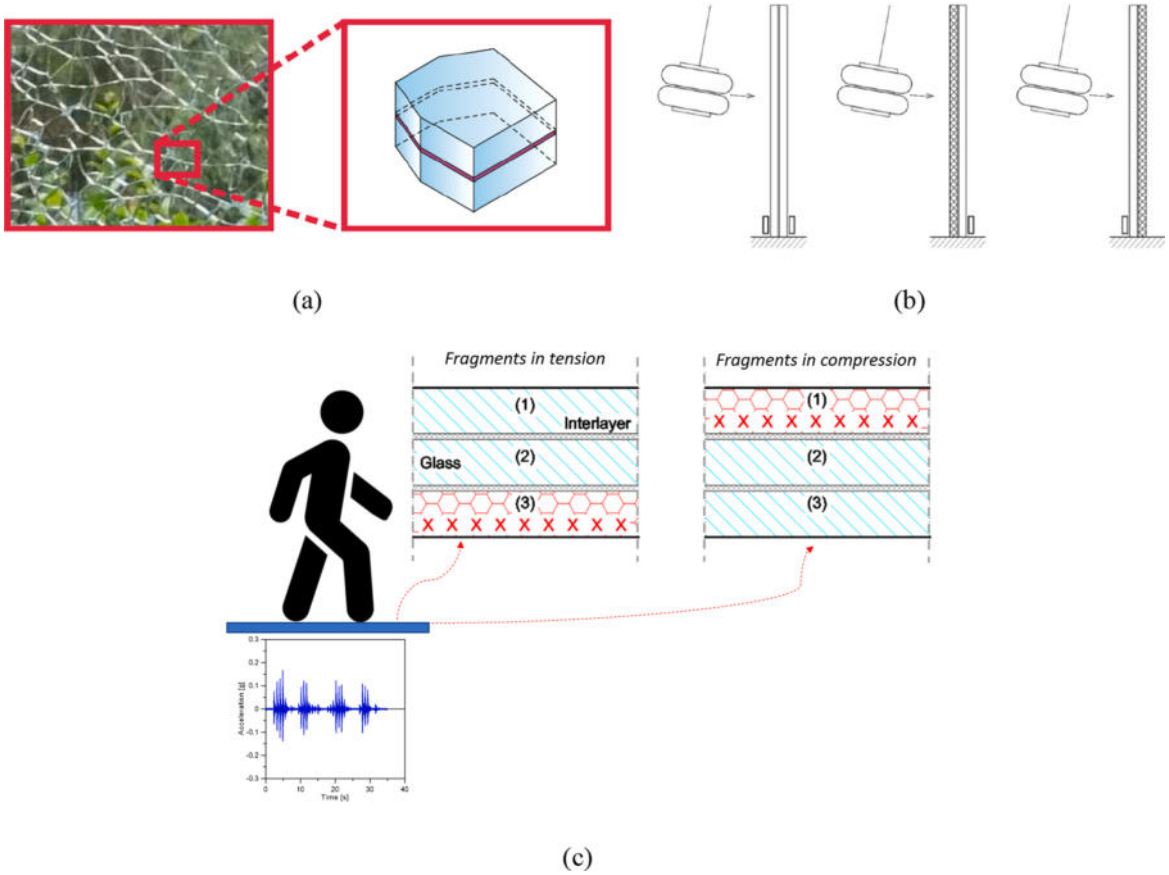

Fig. 1. Post-breakage analysis of laminated glass components: (a) elementary cell for fully fractured tempered glass (figure reproduced from [21] with permission from Elsevier®, Copyright license agreement n. 5260101350166, March 2022); (b) partially fractured LG balustrades (figure reproduced from [8] with permission from Elsevier®, Copyright license agreement n. 5260111418020, March 2022) and (c) schematization of current structural design problem with Collapse Limit State concept for LG pedestrian systems (sacrificial fractured layer).

glass breakage, and thus representing a potential risk to rapidly address for customers. More precisely, the study aims at addressing the potential or limits of time-domain numerical approaches and deterministic models to reproduce walking paths when specifically applied to structural LG components which are characterized by typically high slenderness and flexibility, compared to other slab solutions of typical use in buildings, as well as limited mass, compared to occupants [22–25].

2.2. State of art

The vibration response assessment of glass structures, in the same way of post-breakage considerations, is a relatively recent research topic [26–30], and research in support of design is still needed. As a basic rule, occupied glass slabs should be verified against vibrations in the same way of pedestrian structures composed of other constructional materials [22]. Specific uncertainties and criticalities for in-service pedestrian structures made of glass could be represented by typically small thickness-to-size ratios, limited mass compared to occupants [22], high flexibility and slenderness, unconventional or limited number / size / stiffness of restraints (i.e., point supports, etc.), see [31], the possible / progressive degradation of materials and restraints [32], and even partial glass fracture [25].

For the study reported in [8] and Fig. 1(b), Kozlowski investigated experimentally and numerically the dynamic performance of fully tempered (FT), double LG balustrades under conventional pendulum test. The impact analysis carried out on deliberately pre-cracked LG sections (i.e., one glass layer fractured as in Fig. 1(b)) subjected to twin-tyre setup showed that an isotropic, equivalent MoE for cracked glass layers (E_{fg}, in the following) could be efficiently used to simplify the post-breakage analysis of LG components, in place of the nominal glass MoE ($E = 70$ GPa). In that context, the reference E_{fg} value was experimentally justified and quantified in 17.5 GPa ($\approx 1/4$th the uncracked value E) for fractured glass layers in compression and 2.35 GPa ($\approx E/30$th) for the fractured glass layers in tension from Fig. 1(b). Basic assumption in this equivalent characterization was represented by the knowledge of (p1) mechanical properties for the interlayer in use (with viscoelastic modelling to account for material type, loading, ambient conditions, etc.), (p2) geometrical features of structural components and (p3) experimental structural dynamic response for fitting and model updating.

In this regard, the coupled experimental–numerical frequency analysis and sensitivity investigation presented in [25] for the herein discussed slab modules (and in the specific for the partially fractured module) confirmed that the equivalent MoE approach for fractured glass can represent an efficient approach for post-breakage considerations in partially fractured LG systems, as far as knowledge of (p1) to (p3) parameters is satisfied for model updating. Input values for E_{fg} presented in [25], moreover, were found in close correlation with [8]. This suggests that non-destructive dynamic testing and simple predictive modal analyses carried out to quantify partial glass damage in terms of vibration frequency modification (due to stiffness degradation) could represent a useful procedure for early structural health monitoring and for the derivation of preliminary performance indicators.

2.3. Solving approach

The present study further explores the selected in-service walkway from [25], but discusses original extended numerical investigations in time-domain which are addressed to investigate their potential in the measure of relevant dynamic parameters and damage quantification in LG slabs. More precisely, as in Fig. 2, the study wants to assess:

(i) the potential of consolidated numerical protocols based on the use of deterministic walking loads which are not sensitive to the supporting structure (but they account for general walking features only), and
(ii) the use of numerical output from (i) for the efficient detection of damage in pedestrian LG systems. Compared to other constructional systems, LG slabs are in fact known to manifest higher dynamic modifications when subjected to pedestrians and human-structure interaction phenomena [22–25]. In this sense, differing from in-field or laboratory experimental studies, FE numerical estimates could lack of accuracy for the extrapolation of relevant mechanical parameters on the structural side.

In doing so, a major advantage is taken from earlier experimental studies carried out on a reference LG walkway [22–24], as well as on a preliminary frequency assessment of selected walkway modules affected by partial glass fracture [25]. Rather than on the dynamic identification of structural mechanical parameters as in [22–25], the goal is focused on

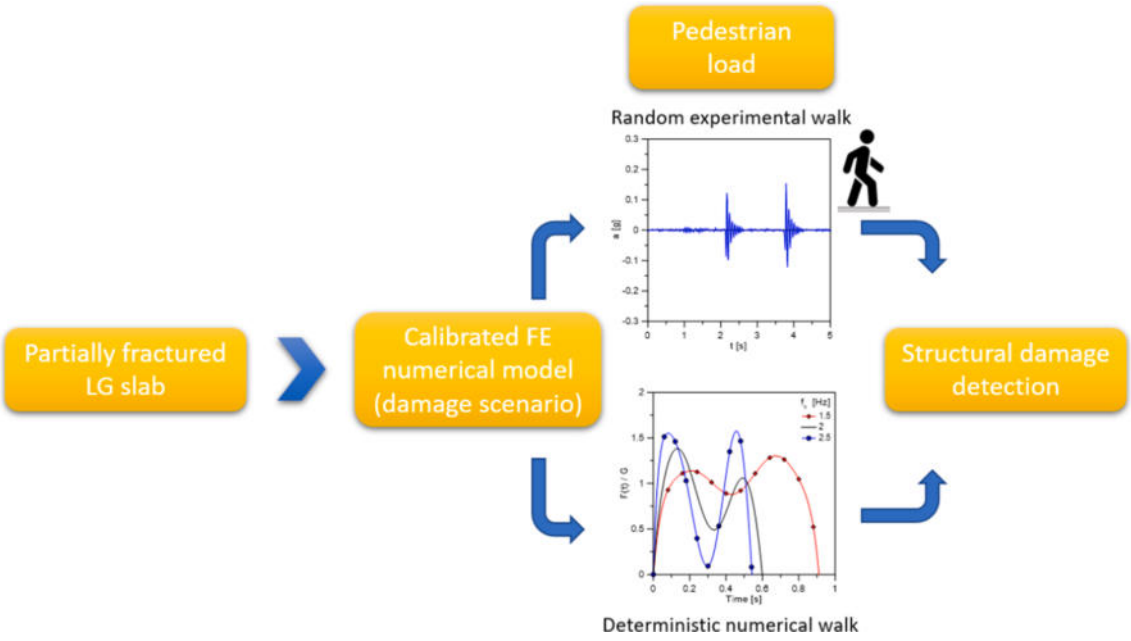

Fig. 2. Reference research methods for the detection of damage in LG pedestrian systems.

the discussion of input mechanical loads on similar structural systems, and on the quantitative measure of expected effects for diagnostic purposes. Earlier validated Finite Element (FE) numerical models are in fact further elaborated in ABAQUS [33], and the attention is given to the analysis of different walking paths to address the effects induced by single pedestrians.

The primary objective, as shown, is to measure in time-domain the sensitivity of vibration and dynamic mechanical parameters for LG pedestrian modules subjected to several walking paths, which are commonly described with consolidated, deterministic models of literature [34,35]. In doing so, a wide set of dynamic analyses is carried out for a LG slab module characterized by intact glass layers (LGU, in the following), as well as on a LG module with identical geometrical properties and boundaries, but suffering for fracture of one glass layer (LGF). Based on the availability of experimental data in support of in-place Operational Modal Analysis for the in-service walkway, the analysis of results from up to 100 simulations is hence focused on the quantification of maximum human induced effects under walking paths, as well as on the verification of time-domain FE model potentials and accuracy to detect and quantify possible damage in similar systems [36].

3. Analysis of vibration parameters due to human-induced interaction

3.1. Experimental operational modal analysis for in-service pedestrian systems

The numerical analysis of human-induced dynamic effects on pedestrian structural components is known to represent a critical issue for design. Generally speaking, consolidated structural health monitoring approaches and procedures in use for the mechanical assessment of constructed facilities and building components confirm that structural system can express any kind of damage in different ways [37,38]. Modal analysis and frequency estimates are for example representative of early damage detection, but many other performance indicators and dynamic parameters could be efficiently taken into account [39–43]. At the same time, it is also recognized that more detailed investigations in which the walking features and the pedestrian interaction with slab modules could be taken into account (Section 3.2).

Such a refined experimental approach can result in difficult application for the vibration and mechanical performance assessment of in-service structural system, where complex experimental protocols could not be allowed to preserve the functionality of the system to analyse. In this regard, the present study takes advantage from Operational Modal Analysis (OMA) techniques and the field experimental analysis of in-service LG modules (Fig. 3). Differing from earlier investigations, the experimental outcomes are used for the validation and assessment of standardized FE numerical procedures in which the structural parameters are derived from time-domain nonlinear dynamic analysis of walking patterns and related effects.

3.2. Deterministic numerical approach

The numerical analysis of human-induced dynamic effects on pedestrian structural components is known to represent a critical issue for design, and several research studies have been focused on the definition of reliable deterministic models to describe pedestrians [44–47].

Literature studies show that human body works as actuator for pedestrian systems [48] and even more for LG systems, due to their intrinsic mechanical properties [49]. Psychological human comfort on transparent / flexible slabs can also further affect the motion features of occupants [50]. When conventional pedestrian loads are applied to LG systems, additional uncertainties can derive from the multiple interaction of geometrical and mechanical properties as in Section 2, and their possible sensitivity (with modification of dynamic parameters) to the motion features (i.e., pacing frequency and phase, walking speed, stride length, etc.).

In the present study, the validated analytical proposal by [34,35] is taken into account, since rather well representative of typical footfall effects due to pedestrians. More precisely, the approach assumes that a single footfall is able to transfer a force time history equal to (in Newton):

$$F(t) = 746\sum_{i=1}^{8} K_i t^i = 746\left(K_1 t + K_2 t^2 + K_3 t^3 + K_4 t^4 + K_5 t^5 + K_6 t^6 + K_7 t^7 + K_8 t^8\right) \quad (1)$$

with K_i the coefficients in Table 1 and t the time (in seconds) within a single footfall, where:

$$t_s = -0.515 f_s^3 + 3.2242 f_s^2 - 6.9773 f_s + 5.8531 \quad (2)$$

denotes the duration of a single footfall (in seconds) of walking frequency f_s (in Hertz). A typical example is shown in Fig. 4(a). The corresponding walking speed is given by:

$$v_s = 1.67 f_s^2 - 4.83 f_s + 4.5 \quad (3)$$

Key parameters to analytically reproduce a realistic walking path as

Table 1
Definition of input coefficients K_i for Eq. (1), based on walking frequency f_s.

	f_s [Hz]		
	≤ 1.75	1.75 ÷ 2	≥ 2
K_1	$-8 f_s + 38$	$24 f_s - 18$	$75 f_s - 120$
K_2	$376 f_s - 844$	$-404 f_s + 521$	$-1720 f_s + 3153$
K_3	$-2804 f_s + 6025$	$4224 f_s - 6274$	$17055 f_s - 31{,}936$
K_4	$6308 f_s - 16{,}573$	$-29144 f_s + 45468$	$-94265 f_s + 175710$
K_5	$1732 f_s - 13{,}619$	$109976 f_s - 175{,}808$	$298940 f_s - 553{,}736$
K_6	$-24638 f_s + 16045$	$-217424 f_s + 353403$	$-529390 f_s + 977335$
K_7	$31836 f_s - 33{,}614$	$212776 f_s - 350{,}259$	$481665 f_s - 888{,}073$
K_8	$-12948 f_s + 15532$	$-81572 f_s + 135624$	$-174265 f_s + 321008$

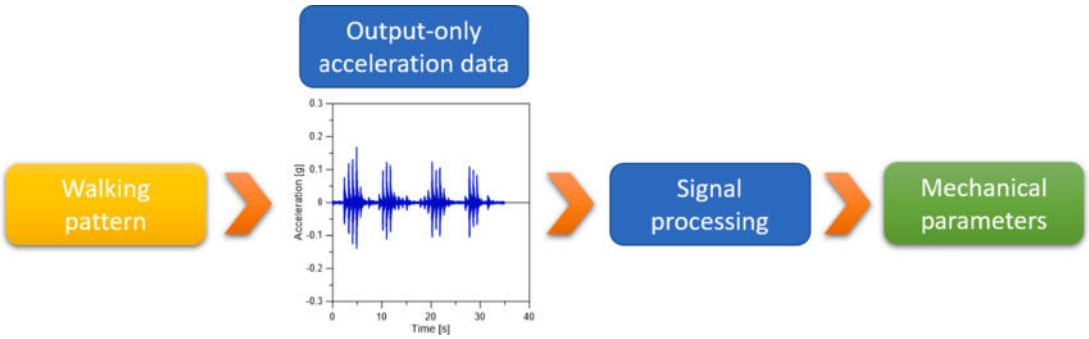

Fig. 3. Classical output-only test setup for Operational Modal Analysis.

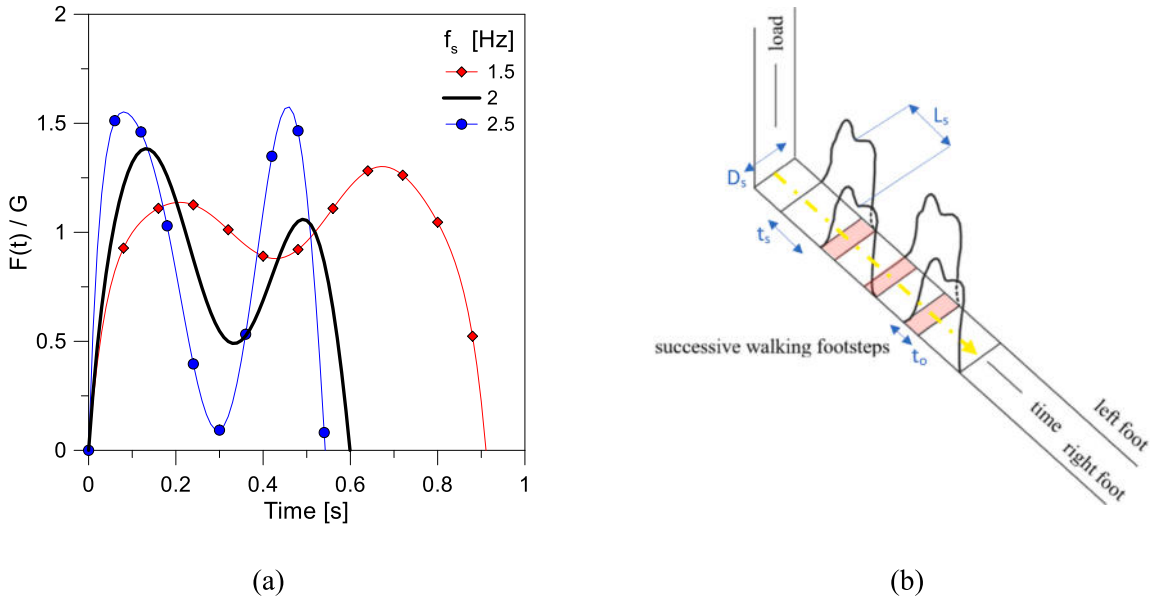

Fig. 4. Description of footfall loads in time based on Eq. (1): (a) typical variation of walking frequency and (b) spatial / timing effects (S#2 and S#3).

in Fig. 3(b) are the possible time overlap of subsequent footfalls (t_o), the length of steps (L_s):

$$t_o = t_s - \frac{1}{f_s} \tag{4}$$

$$L_s = \frac{v_s}{f_s} \tag{5}$$

and the lateral / transversal distance of footfalls ($D_s = 0.2$ m).

Eq. (1), as many others, well reproduces the effects of a "M−shaped" footfall force by accounting for the mass of pedestrian and the walking frequency. Otherwise, the force time history from Eq. (1) is disconnected from the structural parameters of the pedestrian system to verify and design.

Accordingly, the present study aims at exploring the reliability of numerical procedures for the detection and quantification of human-induced effects on slender slab members as it is typical for most of structural glass pedestrian solutions. In the present analysis, three different walking models are taken into account from Eq. (1), see Section 4.

4. Numerical investigation of a case-study LG system

According to Sétra document [51], as also discussed in [31], the investigated structural system can be preliminary classified as "Class III" in-service walkway (footbridge for standard use) from a vibrational assessment point of view. The indoor walkway is in fact composed of independent modular unit with vertical vibration frequency in the order of 13–15 Hz [23–25]. This corresponds to a reference "F4" frequency range in Sétra (greater than5 Hz [51]) which is expected to be associated to "negligible" resonance risk under normal walking conditions.

4.1. Layout and geometry

The reference LG panel has total dimension of 1.35 × 2.65 m (Fig. 5 (a) and (b)). The slab consists of a triple section composed of fully tempered (FT) glass layers (3 × 12 mm) and interposed PVB foils (0.76 mm). An additional protective layer made of annealed (AN) glass (6 mm

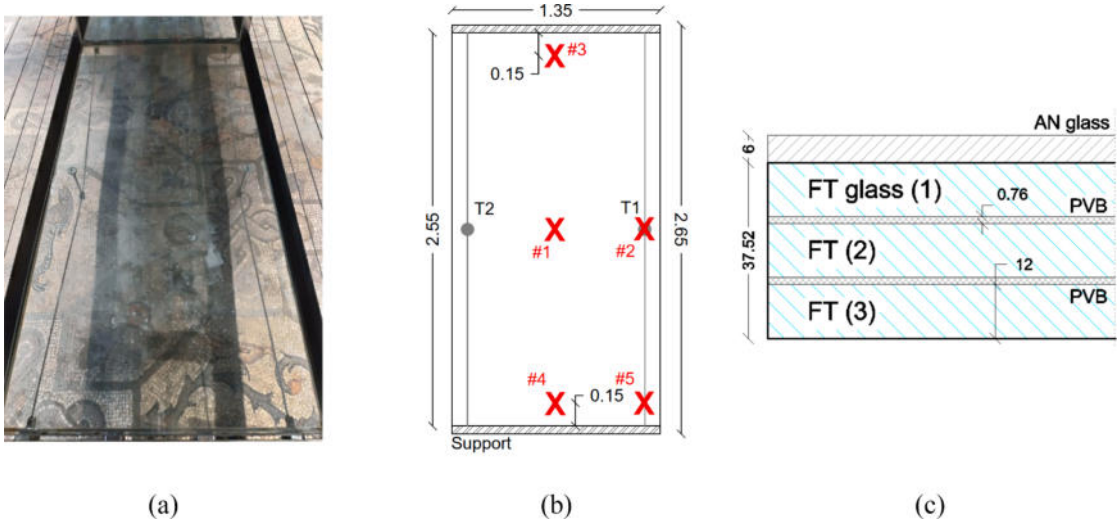

Fig. 5. Case-study LG slab: (a) reference LGU module detail (Crypt of Excavations), with (b) nominal plan dimensions (values in m, with evidence of #*n* measurement points) and (c) cross-section layout (values in mm). Reproduced from [25] under the terms and conditions of CC-BY license agreement.

in thickness) is positioned on the LG top surface (Fig. 5(c)). The mechanical interaction between LG and the top AN layer is offered by contact only. The selected modular units are linearly supported along the short edges. To limit large bending deformations under walking occupants, two pairs of pre-stressed tendons composed of AISI 316 steel are used (10 mm the nominal diameter). Their mechanical interaction with the bottom surface of LG is offered by two unilateral mechanical mid-span point supports only. Two LG modular units are selected for the present investigation. They are part of the indoor pedestrian system serving the Basilica of Aquileia (Italy), and partially experimentally analysed in [22–25]. For the present study, the attention is focused on two original modular units (from a set of 39 elements) that are part of the Crypt of Excavations suspension path (Fig. 6(a)). The difference was represented by the presence of intact glass layers (LGU) for the LG + AN module, or by the presence of one fractured glass layer for the LG section (LGF), see Fig. 6(b). To note that the top LG layer was fractured during maintenance operations, and a carpet was temporarily used to cover cracks, before replacing the LG + AN module.

4.2. Modelling

The numerical investigation of the walkway module was carried out in ABAQUS, in the form of a set of parametric frequency analyses aimed at predicting the fundamental frequency and vibration shape of the structural systems object of study, as well as nonlinear dynamic analyses for more accurate time-domain investigations under human walking patterns.

In doing so, the reference FE numerical model was described based on nominal geometrical and mechanical properties of the system, but also based on the extended calibration of model details that was derived and adapted from [20–23]. A major advantage was in fact represented by knowledge of characteristics of the case-study system, namely consisting in an in-service LG structure with more than 10 years of life and affected by unfavourable ambient conditions [22], thus resulting in rather weak bonding contribution from aged PVB layers [23].

The geometrical layout of the typical modular unit is schematized in Fig. 7. Similar modelling assumptions were taken into account for both LGU and LGF modular units, while the presence of a fractured glass layer was described in the form of material characterization.

A set of “composite” layered shell elements (S4R type) was used for the cross-section of the LG plate (3 × 12 mm glass layers and 2 × 0.76 mm PVB foils) and the sustained AN cover. In this manner, all the constituent layers and materials were separately defined, in accordance with Fig. 6(c). For the unbonded AN glass plate, an additional monolithic layer (6 mm in thickness) was taken into account and placed within the “composite” shell (Fig. 6(c)). To this aim, a thin / soft layer was introduced in-between, so as to account for the actual contact interaction of LG + AN glass (and lack of mechanical fixing).

The final result consisted of a 7-ply shell representative of the LG section (3 glass layers + 2 PVB foils), the top AN cover (1) and the interposed soft bond (1). The typical FE assembly was discretized with a regular mesh pattern having average edge size of 40 mm. Beam elements (B31 type) were used for the steel tendons, to account for their nominal circular section (10 mm the diameter). The FE assembly in Fig. 7 consisted of ≈2000 elements and ≈11000 Degrees of Freedom.

4.3. Boundaries and mechanical interactions

The FE system in Fig. 7 was linearly supported via distributed nodal restraints for the composite shell elements reproducing the LG + AN system. The mono-dimensional steel tendons were also pinned at their ends.

For the point supports at the mid-section of each LG panel, as it can be seen in the box detail of Fig. 7, a unilateral contact interaction was defined for each side, via combined “slot & rotation” connectors. The effect was to reproduce a mechanical point-fixing support able to carry on compressive loads only, but allowing free relative displacements and rotations at the steel-to-LG interface when subjected to tensile / separation loads. Based on an additional “coupling” constraint, such a nodal effect of the coupled mechanical connector was properly distributed onto the whole surface of steel circular plates in Fig. 7 (3 mm their thickness, 40 mm the diameter).

4.4. Material properties

Linear elastic constitutive laws were used for steel, glass and interlayer foils, based on studies earlier discussed for similar modular units of the investigated walkway. The in-field experimental analysis was carried out on the LGF module still affected by glass fracture of one layer. Differing from literature studies voted to explore the coupled pre- and post-breakage response of a given LG system, the present investigation was specifically focused on a damaged setup. As such, the use of linear elastic constitutive laws was justified by expected stress peaks in structural components under walking paths and by the analysis (for LGF case) of a composite section that was already fractured at the time of experiments. The calibrated input values are summarized in Table 2.

A major support for the calibration of PVB bonding layers was taken from the in-service conditions of the studied system, as also discussed in [22–24]. For the LGF module with fractured glass layer on the top of the LG section, an equivalent linear elastic constitutive law was used for FT

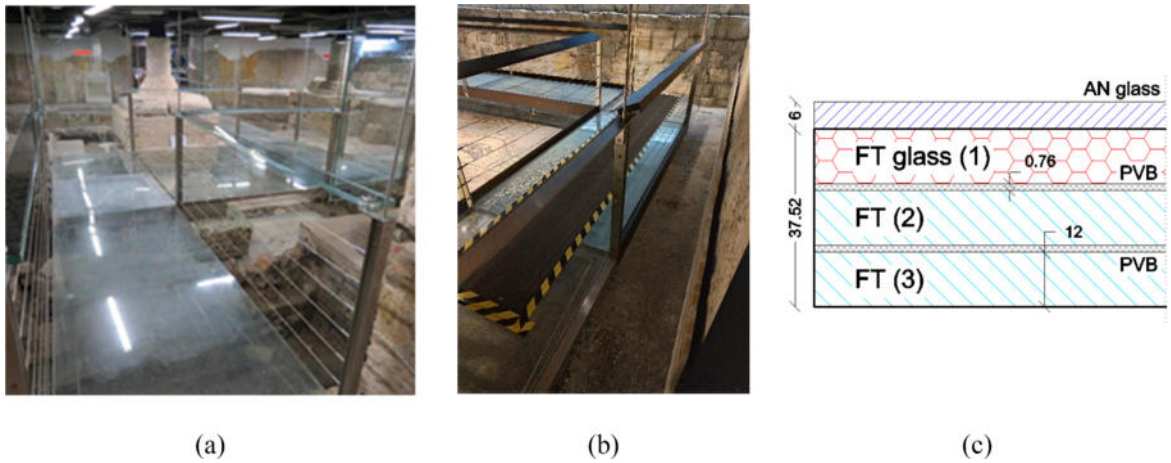

Fig. 6. Operational context for in-field experiments: (a) Crypt of Excavations, with evidence of (b) selected LGF modular unit and (c) corresponding cross-section (values in mm). Reproduced from [25] under the terms and conditions of CC-BY license agreement.

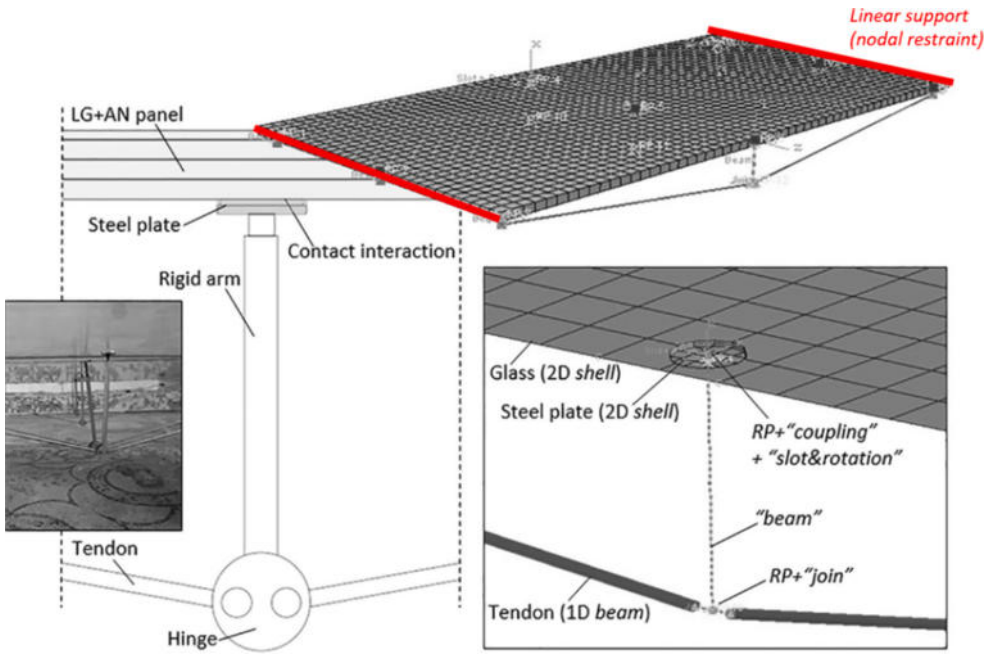

Fig. 7. Assembly concept for the geometrical description of reference FE numerical model (ABAQUS). Adapted from [23] with permission, license order n. 5261980998230, March 2022.

Table 2
Major input material properties for LGU and LGF numerical models.

		Glass	Fractured Glass [25] (LGF – DAM(top) only)	Interlayer [23]	Steel [23]
E	MPa	70,000	17,500	4	160,000
ν	–	0.23	0.23	0.49	0.3
ρ	kg/m^3	2500	2500	1100	7850

fragments, see Fig. 8. More precisely, the anisotropic material option was used for the fractured glass layer in the DAM(top) assembly. Material orientation in the damaged shell layer was set so that the MoE for out-of-plane bending (*x*-*y* plane in Fig. 8) could coincide with $E_{fg} = 17.5$ GPa (fractured layer in compression [25]). The "no tension" material option was used from ABAQUS library. In order to avoid misleading behaviours of the FE model and reproduce the features of FT glass fragments for the composite layout of Fig. 8, the nominal MoE for uncracked glass ($E = 70$ GPa) was used in the vertical direction *z* of material orientation (perpendicular to fractured glass pane).

Regarding the actual LG + AN contact interaction, finally, the shear flexible bond was defined in the form of a fictitious linear elastic material ($E_{SOFT} = 1$ MPa [23]).

Overall, the dynamic performance of LGU and LGF modules under random walks was explored by taking into account the reference cross-sections in Fig. 9(a), so as to quantitatively compare the response of:

- Uncracked (LGU) module,

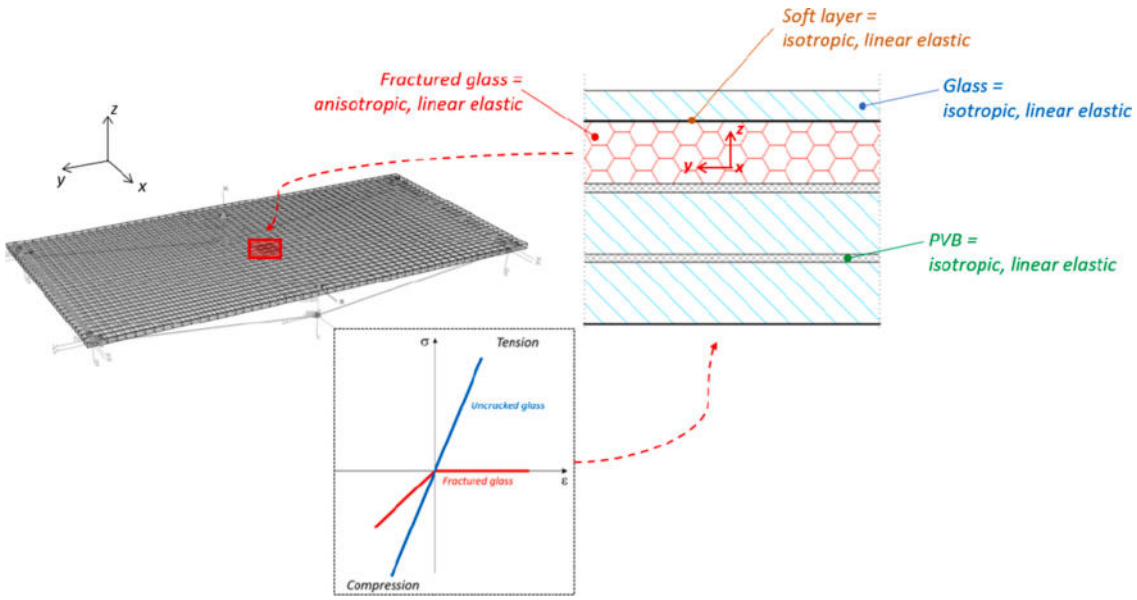

Fig. 8. Material characterization for present DAM(top) model assembly (ABAQUS).

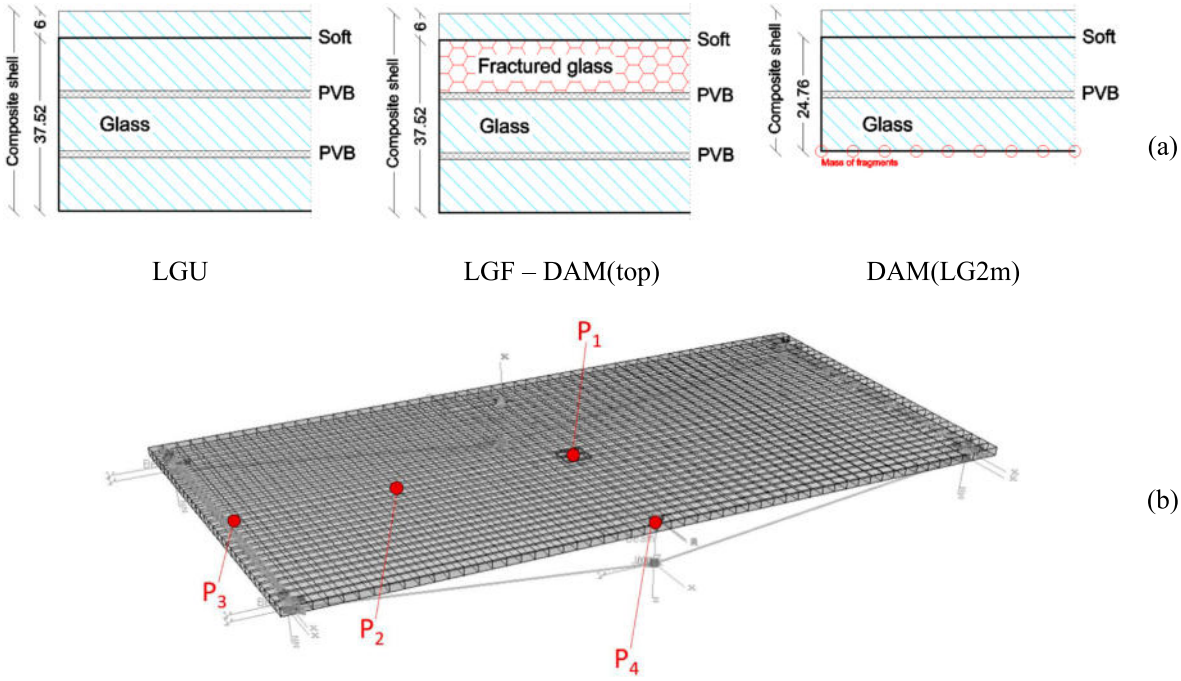

Fig. 9. Numerical approach (ABAQUS): (a) cross-section features (values in mm) and (b) reference control points.

- DAM(top) = Damaged (LGF) modular unit, with fractured glass layer on the top (corresponding to the experimental observation and tested sample in Fig. 6(b), (c)), and material characterization as in Fig. 8,
- DAM(LG2m) = Damaged (LGF) module, being representative of a simplified numerical description of damage characterized by full removal of the out-of-plane stiffness contribution for fractured glass layer and by inclusion of residual mass contribution only for fragments (i.e., $E_{fg} = 0$).

For all the above configurations, the control points P1 to P4 in Fig. 9 (b) were taken into account for quantitative comparison of structural behaviours under random walks.

4.5. Damping

A conventional Rayleigh approach was taken into account to define the mass-proportional and stiffness-proportional damping terms through the parametric numerical analysis [52]. More specifically, they were calculated as:

$$\alpha_0 = \xi \frac{2\omega_1\omega_2}{\omega_1 + \omega_2} \tag{6}$$

$$\beta_0 = \xi \frac{2}{\omega_1 + \omega_2} \tag{7}$$

where ω_1, ω_2 are the natural circular frequencies corresponding to first and second vibration modes of the examined system. Given that the LGU and LGF modular units proved to have different vibration frequencies in the experimental and numerical analysis from [25], this means that the damping terms from Eqs. (6) and (7) were separately calculated for each one of the investigated FE configurations. In doing so, a conventional 2

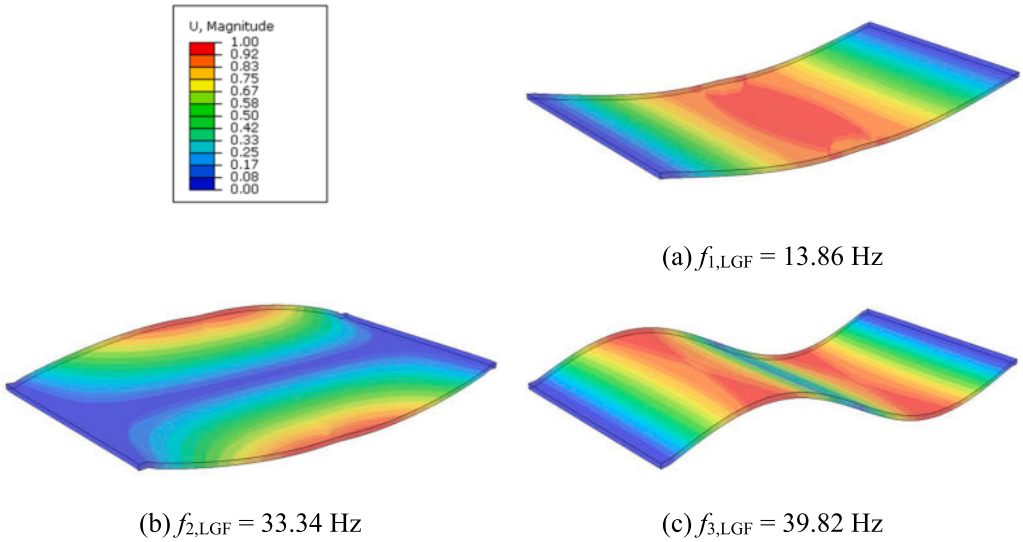

Fig. 10. Vibration modes of the reference modular unit: (a) first, (b) second and (c) third vibration shape (ABAQUS, with glass components in evidence).

% damping term was initially considered. To note that such a damping value is also in line with average experimental damping estimates presented in [24] for similar modular units of the case-study walkway, under single pedestrian walks. Typical vibration shapes are shown in Fig. 10 (with glass components in evidence), were the corresponding frequencies (example for the occupied LGF module) are also proposed.

5. Experimental feedback, model validation and loading protocol

5.1. *In-field experiments*

To assess the FE numerical predictions of the LGU and LGF model

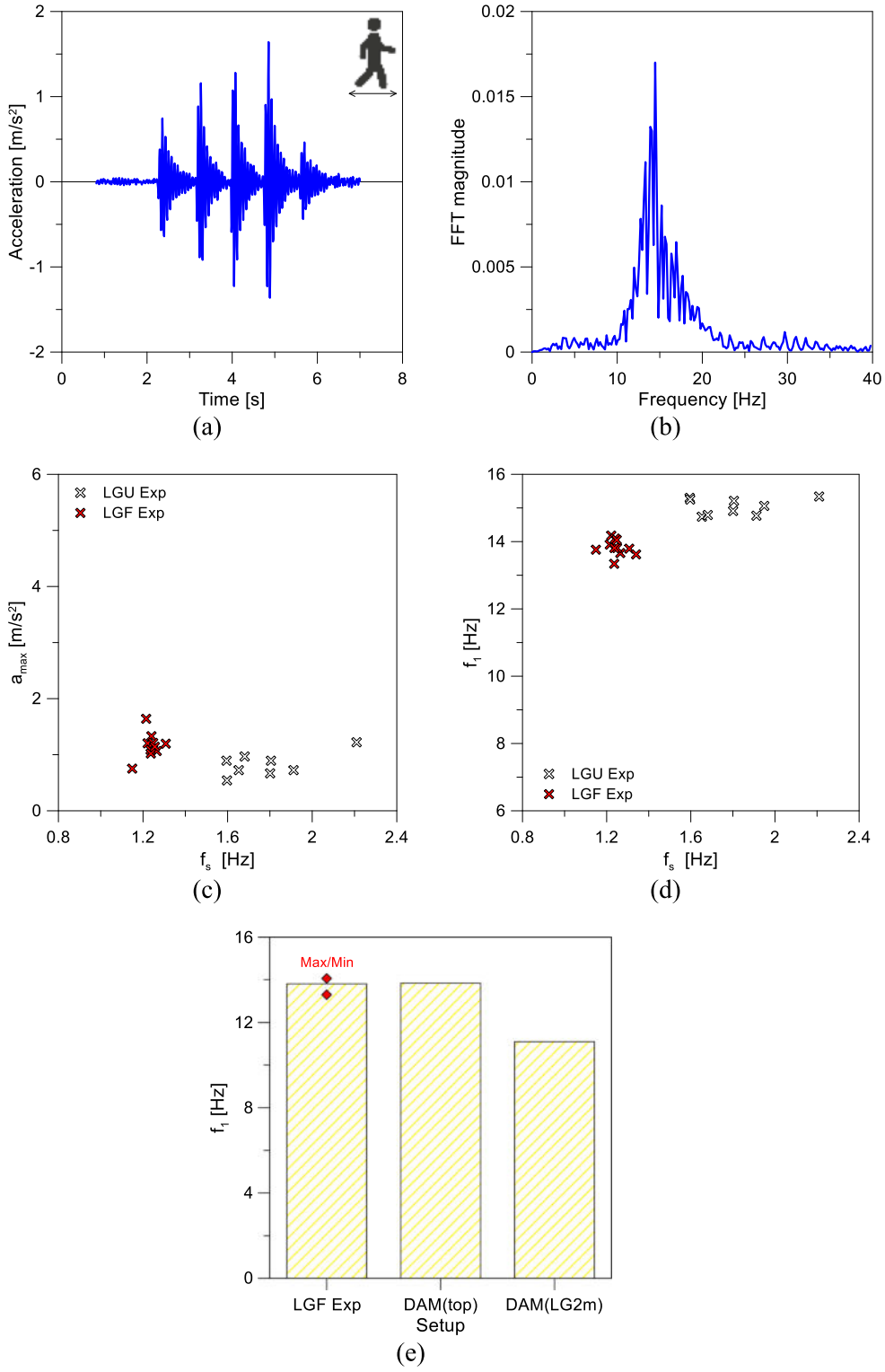

Fig. 11. Example of linear walking paths: (a) vertical acceleration record and (b) corresponding FFT magnitude main, with (c)-(d) summary of calculated dynamic parameters for the experimental records considered in the present study and (e) preliminary frequency assessment for the occupied LGF module. Figures (a) and (b) adapted from [25] under the terms and conditions of CC-BY license agreement.

assemblies calibrated to previous literature studies, a specific advantage was taken from the availability of experimental records which have been collected during the in-field investigation performed in August 2021.

A single tri-axial Micro Electro-Mechanical Systems (MEMS) accelerometer was used [53] and the on-site investigation program was deliberately focused on selected LG + AN modules according with Figs. 5 and 6, that is identical global dimensions, boundaries and cross-section layout / composition, but the presence of intact (LGU sample) or partially fractured (LGF) glass layers. A single occupant ($M = 80$ kg the weight) was invited to take part in measurements on LGU and LGF modules. Output-only tests data were collected under the effects of normal walks or in-place jumps. For the investigation in object, the sampling rate was set in 100 Hz. The typical record was characterized by a maximum duration of ≈2 min. During random walks, a single MEMS sensor was repeatedly moved on the slab, so as to capture the acceleration time histories from control points #1 to #5 schematized in Fig. 5 (c). Basically, due to limited size of each LG + AN module, most of the walking configurations included linear paths along the midline of each module (i.e., a total of 4 steps as in Fig. 12). In-place jumps were imposed at the centre of LGU and LGF modules. For the herein presented analyses, experimental records measured in #1 were only considered. Moreover, due to the fact that the experimental measures were collected in the Basilica without functionality interruptions, but also due to some uncertainties on the residual capacity of LGF modular unit, walk patterns were characterized by average frequency in the order of $f_s \approx 1.3$ Hz, that is slightly lower than a conventional walk ($f_s = 1.5$–2.5 Hz).

A typical example of experimental records selected from [25] is shown in Fig. 11. Moreover, Fig. 11(c) and 11(d) summarize some calculated walk parameters (vertical acceleration peak a_{max} and vibration frequency f_1 of the occupied system), as a function of walking frequency f_s. In this regard, it is worth to note that maximum acceleration peaks under random walks never exceeded the top value of 2.4 m/s^2. In accordance with recommended performance indicators by Sétra [51] for vibration serviceability assessment, the calculated acceleration peaks in Fig. 11(c) and (d) would correspond to "minimum" comfort level for occupants (with 1–2.5 m/s^2 the reference acceleration range, "A3"). Besides, such a discomfort against vibrations was not confirmed by the involved volunteer [22]. The experimental measurements were post-processeed and preliminary analysed in [25] with the support of SMIT Toolsuite [54], in order to detect the fundamental vibration frequency of the structure object of study. The test setup and experimental protocol was in fact optimized based on the previous investigation [24], where some LG modular units of the case-study walkway have been previously explored. In the post-processing stage, the ERA-OKID-OO approach was used [55,56].

Worth to note in Fig. 11(d) that the average vibration frequency of LGF and LGU modules was experimentally calculated in [25] in $f_{1,\mathrm{LGF}} = 13.8$ Hz (±0.21 Hz) and $f_{1,\mathrm{LGU}} = 15.05$ Hz (±0.2 Hz) respectively, thus manifesting down to a mean −8.3% of frequency decrease due to damage. Model updating based on simple frequency analyses was then proposed in [25] to assess the potential stiffness contribution of the fractured glass layer, based on the equivalent E_{fg} concept and on the fundamental vibration frequency sensitivity as a major early warning parameter (Fig. 11(e)). Further, modal correlation was carried out in [23] for uncracked modular unit and a similar FE modelling approach, giving evidence of rather good Modal Assurance Criterion (MAC) estimates.

Besides, no detailed walking features were taken into account in [23] or [25] in terms of structural analysis for the occupied system under random configurations. The present analysis starts from material calibration in [25] to investigate the mechanical response of the system in time-domain, under a wide set of walking paths.

5.2. Solving approach and loading strategy

Special care was given to the nonlinear dynamic analysis of walkway modules under pedestrian loads.

Three different walking paths were taken into account. The first approach consisted in a simple simulation procedure (S#1, in the following) in which the footfalls were imposed at the centre of slab module. No spatial and time variations of subsequent footfalls (4 in total) were taken into account in the time-domain nonlinear dynamic analyses (Fig. 12(a)).

In the second case (S#2), a more realistic loading scheme was considered, and 4 subsequent footfalls according to Eq. (1) were considered for the examined slab module (Fig. 12(b)). More precisely, as also in accordance with [47], a spatial variation $D_s = 0.2$ m was included in the transversal direction. For the longitudinal direction, the overlap time t_o was also introduced between subsequent footfalls. The distance L_s of subsequent footfalls was set with "footfall 1" positioned close to the lateral supports of the slab module.

Finally, the third configuration (S#3 in Fig. 12(c)) was derived from S#2, with the difference that "footfall 2" and "3" were symmetrically centred with respect to the middle point of the slab module. Accordingly, "footfall 1" and "4" were positioned at a longitudinal distance L_s.

The third set S#3 was taken into account to assess possible sensitivity of slab vibrations and performance indicators to walking features (footfall position).

For the so-defined S#1 to S#3 schemes, the walking frequency f_s was modified in the range from 1.5 Hz to 2.5 Hz (0.1 Hz the variation step). A reference footwall with 10 cm × 10 cm was used to uniformly distribute the load-time function as in Eq. (1) and Fig. 12. The integration time of analyses was set in 0.005 s, that is two times the sampling rate of experimental records.

6. Discussion of parametric numerical results

6.1. Performance indicators

The analysis of parametric numerical results was focused on different aspects for vibration detection. First the vertical acceleration peaks and corresponding deflection values were detected for the LGU and LGF modules under various walking conditions.

For the discussion of parametric results, the attention was focused on control points in Fig. 9(b) and on the analysis of vertical accelerations in time and deflections. Major attention was paid for walking schemes S#2 and S#3, due to the time and space variability of footfalls. The typical effect on glass (vertical accelerations in evidence) can be seen in Fig. 13. A preliminary look at principal stresses in glass was also taken into account to ensure a linear elastic performance of glass panels. Besides, limited stress peaks were generally observed in time-domain.

The typical comparative analysis can be seen in Fig. 14 for the LGU (uncracked) model under variable walking configurations. Worth to note the variation in time history content and amplitude, as a function of conventional walking loads as defined in Eq. (1) for a selection of S#1, S#2 and S#3 schemes.

Minimum variations in performance indicators were generally measured for schemes S#2 and S#3, even under different walking frequencies f_s. This means that localized position of footfalls for the present modular units has no marked effects for mechanical and vibration issues. Accordingly, simplified numerical protocols may also be taken into account for human-induced effects.

Worth to note that the S#1 scheme, as far as performance indicators are examined in the central control point P1, are largely pronounced compared to S#2 and S#3 effects in Fig. 14, thus confirming the need of various control points and maximum envelope considerations to quantify the dynamic effects on the slab modules. For this reason, comparative data were considered as envelope outcomes of the parametric numerical study herein discussed.

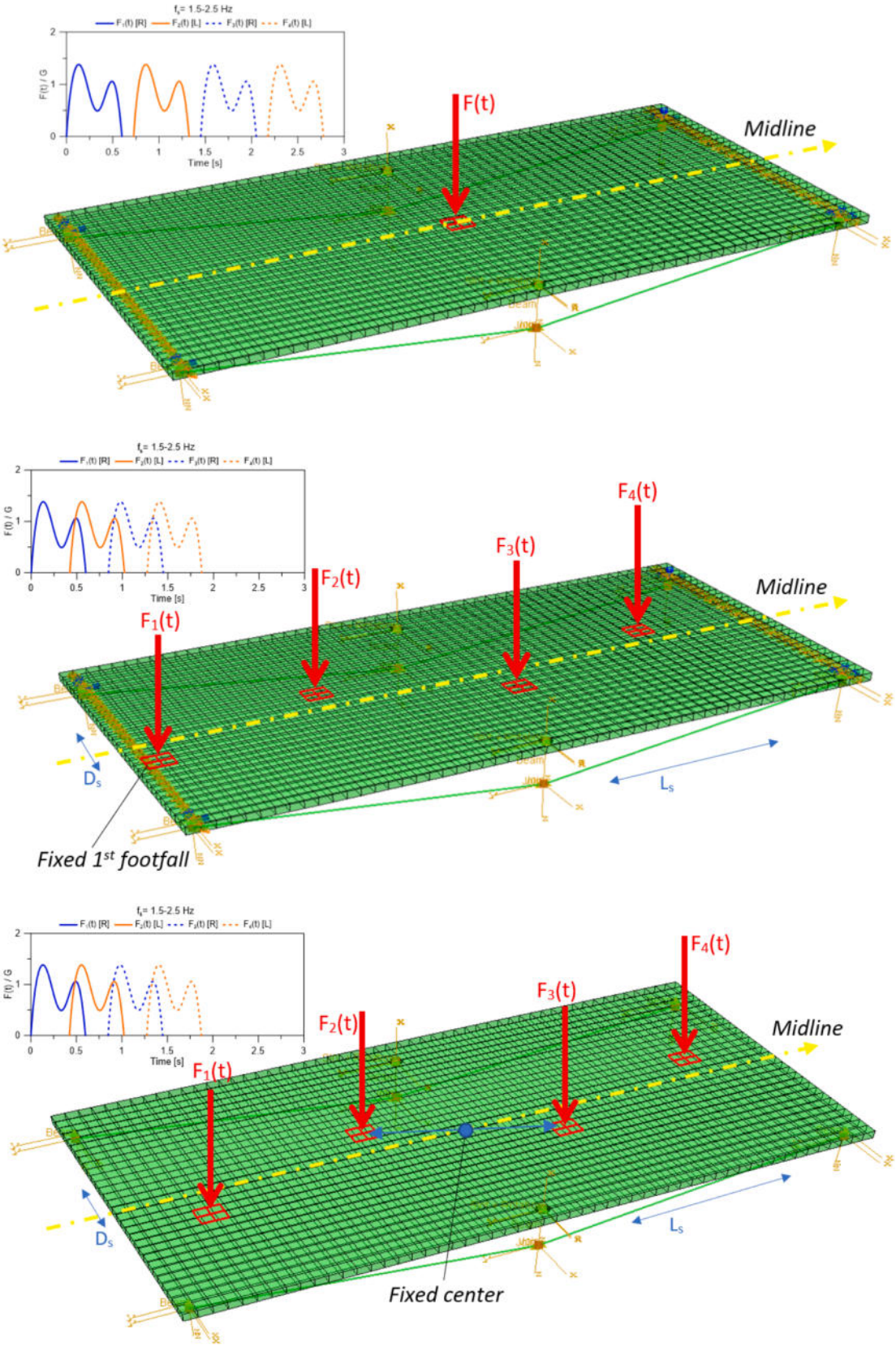

Fig. 12. Adopted loading schemes: (a) S#1, (b) S#2 and (c) S#3 walking paths (ABAQUS).

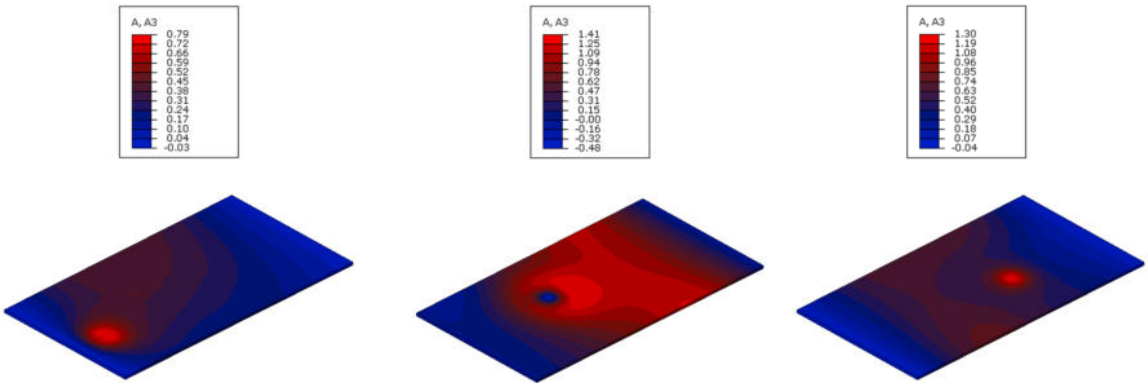

(a) Footfall 1 (b) Footfall 2 (c) Footfall 3

Fig. 13. Numerical analysis of slab modules under S#3 walking conditions, with evidence of local acceleration peaks in glass at selected time instants (ABAQUS, values in m/s^2).

6.2. *Sensitivity of performance indicators to walking conditions and damage*

The analysis of numerical results was first examined in terms of time-domain parameters and maximum performance indicators, for various walking paths and both uncracked or fractured glass layers. Typical examples can be seen in Fig. 15 and confirm a certain sensitivity, as also expected, of monitored data. In doing so, the attention was focused on S#1 and S#2 schemes, given that minor modifications were generally observed between S#2 and S#3 scenarios.

Figs. 16 and 17 show selected results for S#1 paths and the LGU or LGF modules, together with DAM numerical configurations. In general trends, the higher walking frequency fs was found to manifest in increasingly amplitudes for vertical acceleration and deflection. Such an outcome strictly depends on the fundamental vibration frequency of LGU and LGF modules. As a result, the higher is fs and the higher are the measured vibration parameters. Clearly, current outcomes cannot be generalized to draw conclusions, but the focus of present study is to use the available comparative data to possibly quantify the expected effects of combined damage and conventional walking paths.

Most importantly, it can be noticed a different sensitivity and numerical interaction of damage scenarios with walking configurations. The LG2m module, which is the most conservative of numerical damage scenarios (i.e., removed fractured glass layer), is also associated to lower and unrealistic vibration frequency f_1. The interaction of multiple aspects results in a LG2m damage condition which is the most flexible compared to others, and related to large deflections (≈-68% ±13.3 the average deflection increase under various S#2 walking paths, compared to LGU). On the other side, even compare to the uncracked model, the LG2m module is not necessarily associated to maximum absolute peaks of vertical acceleration and deflection for the imposed walking paths.

Regarding the DAM(top) approach for the LGF module, finally, it can be seen in Figs. 16 and 17 that appreciable variation of maximum deflection was typically observed compared to the LGU system (≈-6% ±4.6 the average deflection variation under various S#2 walks). Accordingly, a numerical monitoring of maximum deflections in time – based on conventional walking paths and features – may result in difficult quantification of mechanical damage.

6.3. *Accuracy of numerical walks to predict human induced accelerations*

As far as the acceleration peaks are taken into account as a function of walking frequency f_s for several paths, see Fig. 18, the parametric numerical data can be easily compared with experimental outcomes. The attention is focused in Fig. 18(a) on the uncracked LGU module, where experimental data derived from variable walks an P1 acceleration measures are taken into account. Worth to note is the general good trend of a_{max}-f_s data with numerical predictions. S#1 numerical configurations, more precisely, largely overestimate the actual acceleration peaks that the uncracked LGU module is expected to suffer. A good trend can be indeed noticed between variable S#2 walks and corresponding experimental peaks in P1.

In case of LGF module, comparative data are collected in Fig. 18(b) to (d), grouped by walking paths. Worth to note, in this case, that experimental data are obtained from various control points and are not limited to P1. This justifies the sensitivity of experimental accelerations to rather small walking frequency variations. As far as numerical results from Fig. 18(c) and (d) are taken into account (envelope), it is possible to see that experimental peaks are within the top numerical trend from dynamic analysis. A major sensitivity can be noticed in presence of damage. Besides, a still good trend of comparative results can be observed. Also in this case, the use of S#1 walking paths as in Fig. 18(b) tends to overestimate the acceleration peaks for the numerical model, and should be limited to preliminary estimates and considerations only.

Finally, see Fig. 19, the use of a simplified LG2m approach would act on the conservative side in terms of envelope of effects due to numerical walking paths, but overestimating the actual numerical response.

6.4. *Accuracy of numerical walks to predict human induced frequency variation*

In conclusion, the acceleration time histories collected from the parametric numerical analysis were used for signal processing of FE outcomes, as it is usually done in case of experimental protocols. The post-processing methodology was carried out as described in Section 5, with the exception that the output-only analysis was based on numerical time-acceleration records. In this manner, the vibration frequency of examined slab modules was calculated and compared in terms of damage sensitivity for the LGF or LGU conditions (% scatter). Typical results are proposed in Fig. 20, by taking account the walking frequency modification. Evidence is given also to the average frequency decrease that was measured in [23] (and recalled in Section 5) for the fractured LGF module.

It is possible to see in Fig. 20(a) that frequency scatter is not uniform with f_s, and for some walking paths is close to zero. Major frequency variation is mostly obtained for the S#2 walking paths rather than for various in-place S#1 schemes. Moreover, low frequency walks (f_s = 1.5–1.6 Hz) are numerically associated to f_1 decrease in the order of ≈-6%, which tends to the mean experimental value of −8.3%. This is not the case of S#1 scenarios, which are mostly associated to rather small frequency sensitivity, even in presence of damage.

In Fig. 20(b), a similar comparison is presented for the simplified

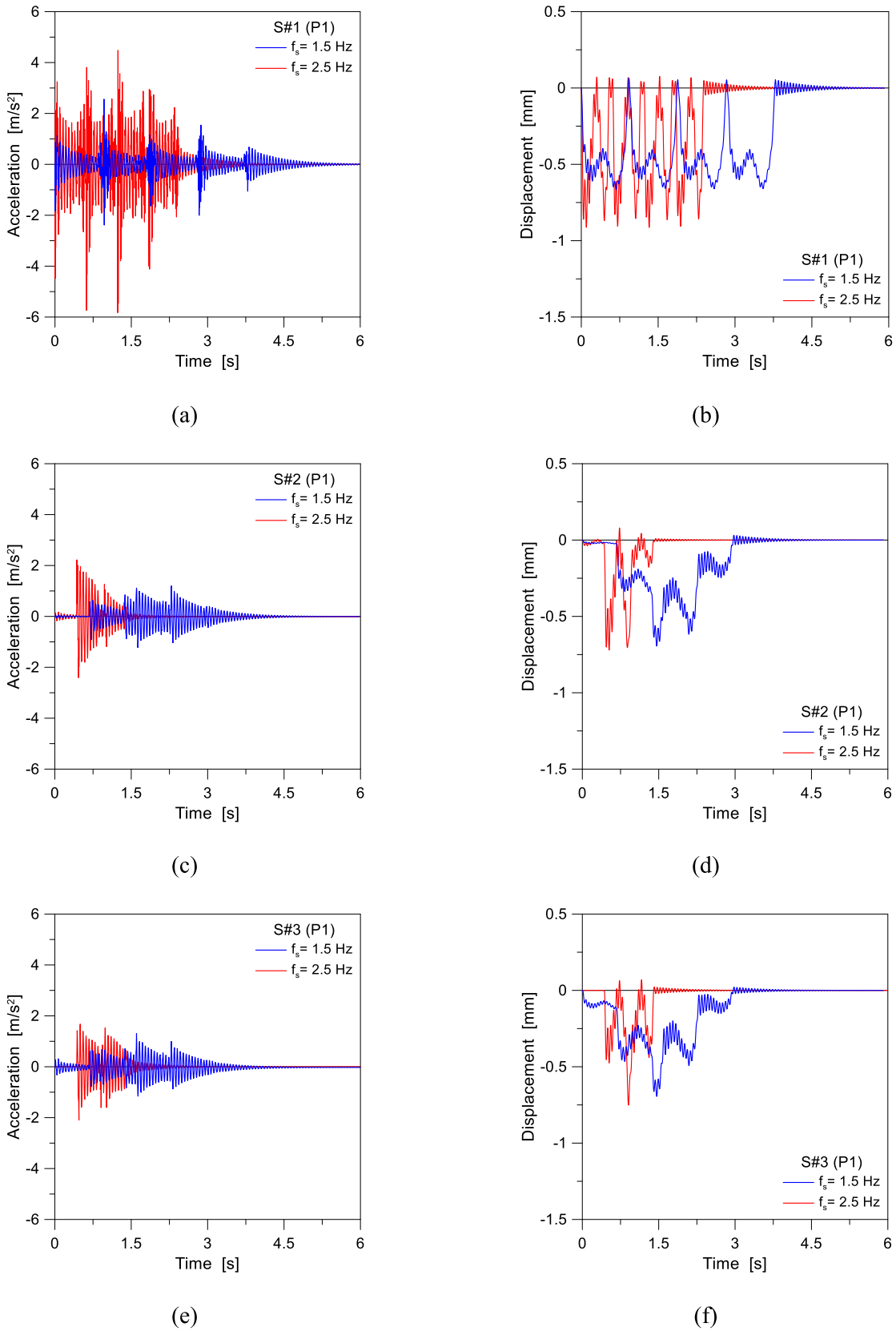

Fig. 14. Numerical analysis of uncracked LGU module under various walking conditions: (a)-(c)-(e) acceleration and (b)-(d)-(f) displacement in time, for selected walking paths S#1, S#2 or S#3 (ABAQUS).

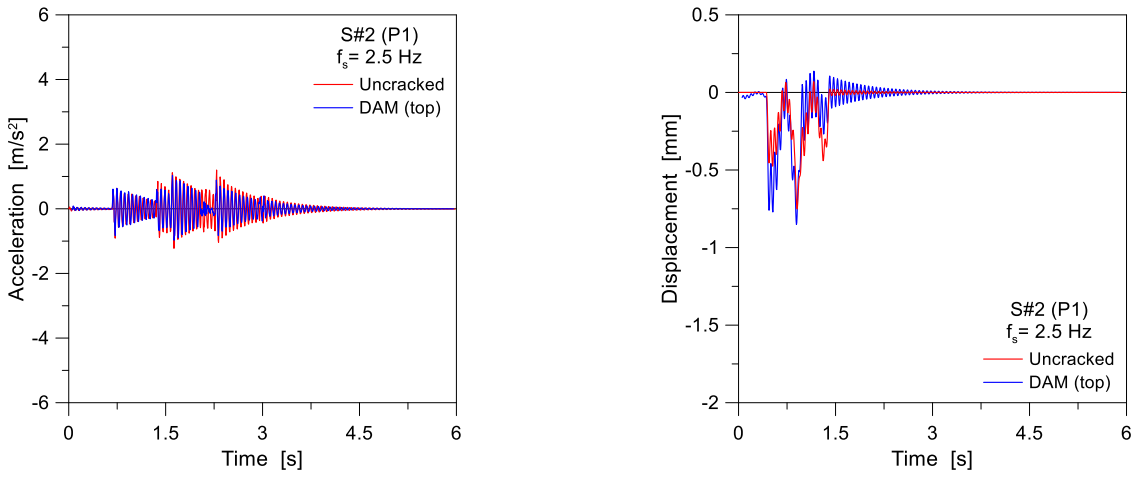

Fig. 15. Numerical analysis of LGU of LGF modules (DAM(top)) under selected walking condition: (a) acceleration and (b) displacement in time (ABAQUS).

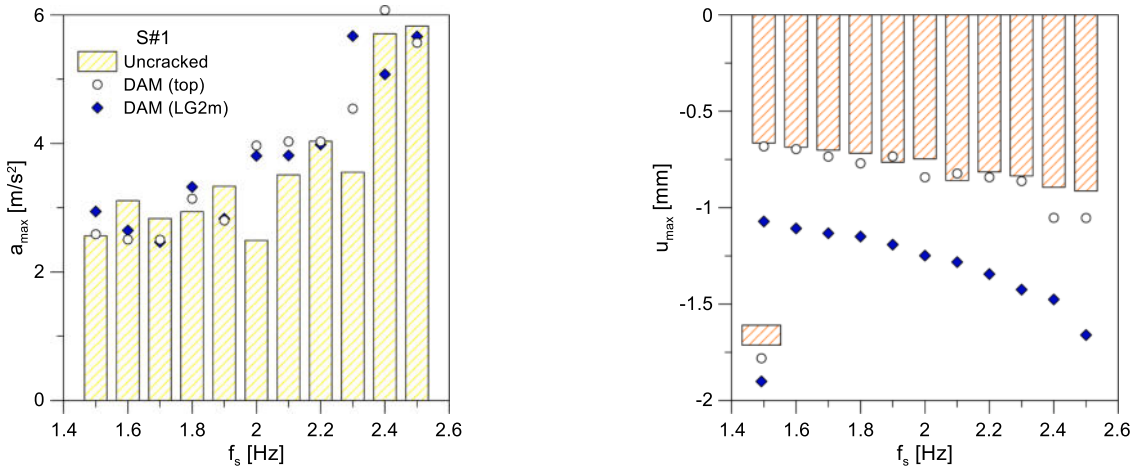

Fig. 16. Numerical analysis of LGU or LGF modules under various S#1 walking conditions: (a) vertical acceleration peak and (b) maximum deflection (ABAQUS).

LG2m modelling approach. As expected, the calculated scatter for LGU and LGF conditions looks numerically higher than in Fig. 20(a), down to ≈-25%. Furthermore, less sensitivity to S#1 or S#2 walking paths can be noticed in Fig. 20(b), as far as f_s modifies. In any case, the measured vibration parameters look largely overestimated, compared to the experimental outcomes. This confirms that the LG2m procedure for collapse prevention is on the conservative side for design purposes but roughly efficient in reproducing the actual performance of fractured LG members, thus underestimating the post-breakage residual capacities of glass fragments.

Knowledge of numerical response and performance indicators for LGU and LGF modules can suggest to introduce a further parameter:

$$R_X = \frac{X_{LGF}}{X_{LGU}} \tag{8}$$

in which the measured performance indicator X can be compared for the fractured or uncracked module (maximum value), as a function of vibration frequency variations from Fig. 20, under various walking conditions. In this regard, Fig. 21(a) and (b) show the acceleration peak increase, as a result of damage in glass (and modification of mechanical / dynamic parameters for the slab module under walking paths), while Fig. 21(c) gives evidence of deflection variations, for various walking paths.

As far as the central control point P1 is taken into account, the measured vertical acceleration peak is slightly sensitive to walking conditions, while major effects are given by damage description for the fractured glass (and thus frequency modification compared to LGU). Besides, the analysis of envelope accelerations for damaged slabs as in Fig. 21(b) confirms the high sensitivity of the examined LG solutions to walking paths characterized by time and space variability. Compared to the LGU condition, fracture of one glass layer can result in up to ≈2-3 times the expected acceleration peaks under ordinary walking paths.

Finally, Fig. 21(c) shows a rather limited variation of P1 deflection due to human induced effects for movable walking loads as in S#2 (or S#3) schemes.

7. Summary and conclusions

The post-breakage performance assessment of structural glass elements is a critical issue for design, and especially for structural members

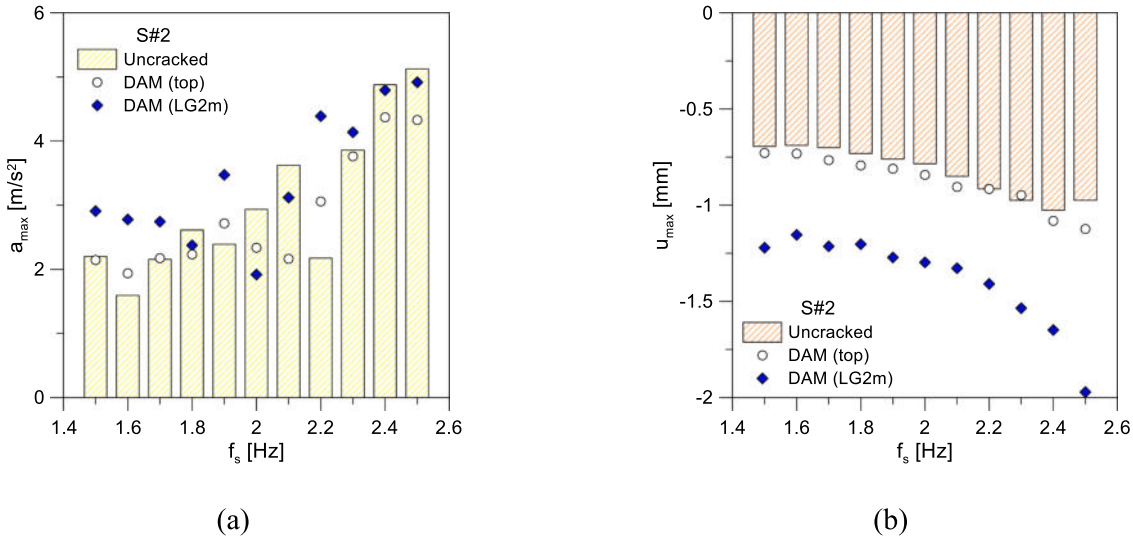

Fig. 17. Numerical analysis of LGU or LGF modules under various S#2 walking conditions: (a) vertical acceleration peak and (b) maximum deflection (ABAQUS).

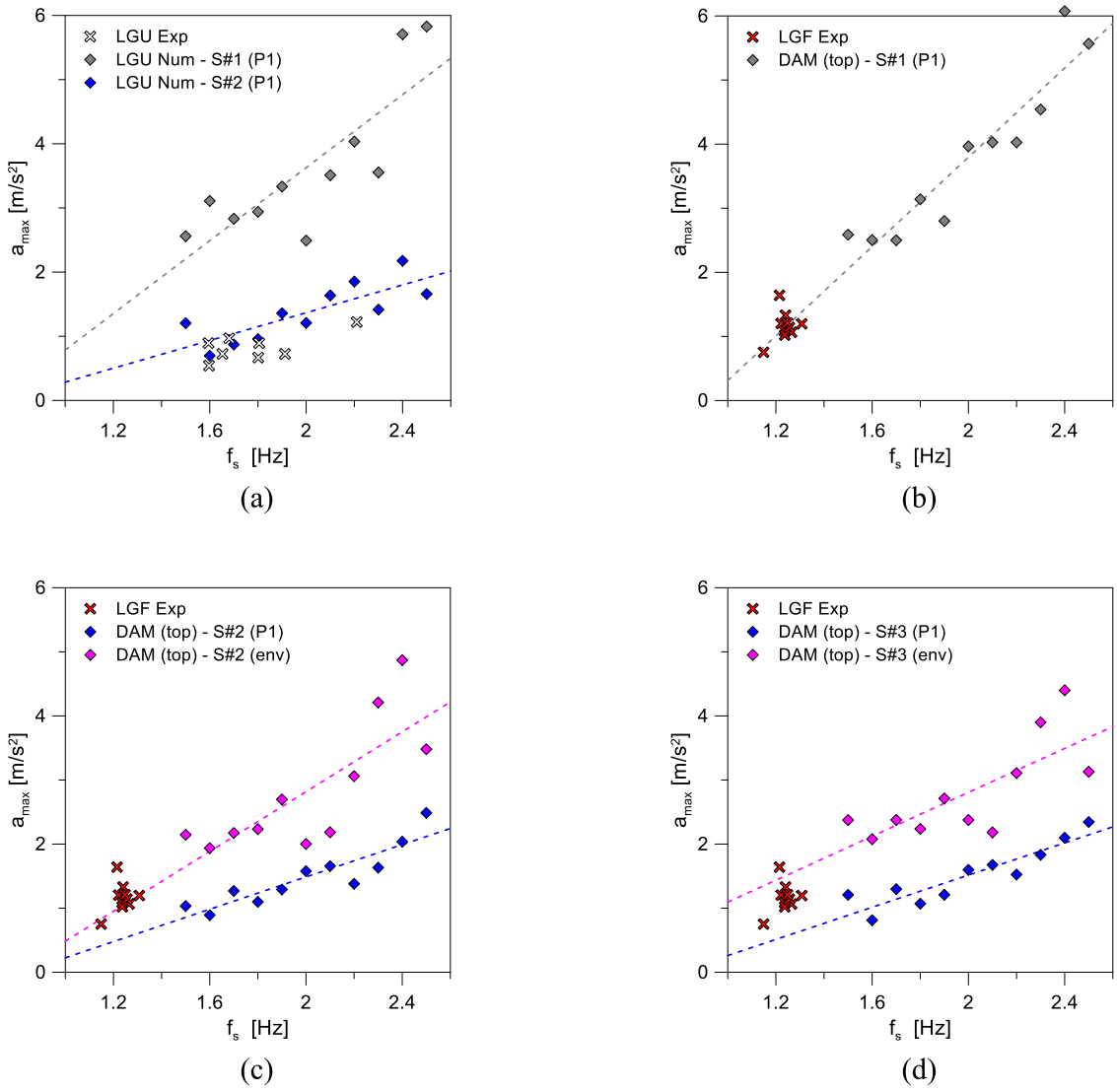

Fig. 18. Numerical analysis of LGU or LGF modules under various S#1, S#2 and S#3 walking conditions (vertical acceleration peak, ABAQUS).

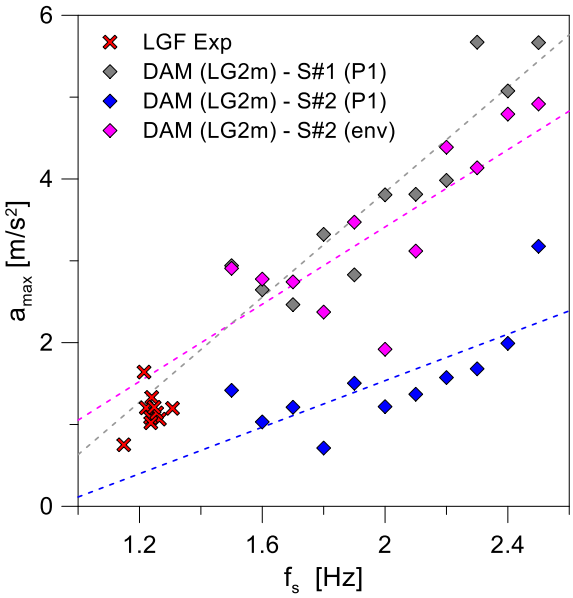

Fig. 19. Numerical analysis of LGF module under various S#1 and S#2 walking conditions (vertical acceleration peak, ABAQUS).

which are expected to suffer for direct interaction with customers, as pedestrian systems. Due to intrinsic material properties, boundary conditions and operational configurations for laminated glass (LG) elements, a multitude of aspects should be in fact considered on the structural side. Furthermore, sensitivity to vibrations may be addressed under random walks. In this regard, dedicated experimental protocols would generally efficiently support design and retrofit decisions and considerations. On the other side, experimental methods are often not available or difficult to arrange, especially for in-service structures.

In the present study, the attention was focused on the vibration analysis of in-service LG modular elements belonging to an indoor, case-study pedestrian system built in Italy, affected by more than 10 years of life and suffering (August 2021) for partial fracture of the constituent glass components when subjected to ordinary walking conditions.

A major advantage was taken from an extended set of nonlinear dynamic simulations carried out with the support of Finite Element (FE) numerical models calibrated to earlier vibration experiments A special attention was preliminary given to fundamental frequency estimates, given that they represent a rough but still rather exhaustive parameter for structural health monitoring and early maintenance purposes. The vibration performance indicators (including damage) were then numerically assessed by means of several walking paths and pedestrian loads from a single individual, which were analytically described with consolidated approaches of literature.

From the present study, the following conclusions can be derived:

- Any kind of material degradation or damage in LG slabs is typically associated to marked variation in mechanical performance indicators, such as vibration frequency, acceleration peaks, deflections. Early monitoring studies can be thus carried out based on quantitative comparison of classical indicators. For the present study, for example, fracture of one of constituent glass layers was quantified in ≈-8.3% fundamental frequency decrease under random walks, compared to the intact in-service system (see Fig. 11(e)).
- The analysis of damage scenarios based on geometrically simplified numerical models in which the fractured glass layers are fully disregarded in terms of residual stiffness (as it is design in practice, in accordance with existing design guideline documents for Collapse Limit State prevention) was found to result in largely conservative estimates of mechanical response parameters, and also to strongly underestimate the actual post-breakage capacity of experimental modules, up to ≈68% variation in terms of deflection (see Fig. 17).
- The use of deterministic analytical models of classical use to describe walking paths and pedestrian loads (which is known to disregard the mechanical and dynamic features of supporting structure, and possible local interaction), the numerically predicted structural response may not capture the real dynamic behaviour under human induced effects. For the presently investigated LG slab modules (see for example Fig. 18), the use of similar loading procedures was associated to structural dynamic estimates that both underestimated or overestimated the available in-field experimental results on the structural side.

Moreover, from the numerical investigation it was shown that:

- Acceleration peaks in time-domain analysis should be predicted by deterministic load patterns in which time and space variability of footfalls is taken into account (i.e., S#2 or S#3 walking schemes, rather than S#1);
- Multiple control points should be taken into account to quantify human-structure interaction effects on slender LG slabs, rather than a

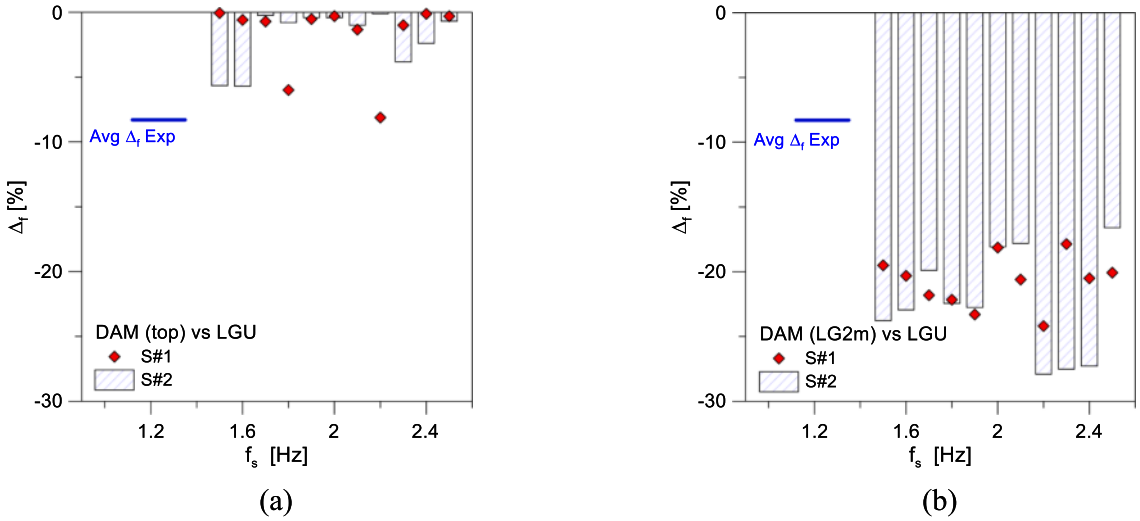

Fig. 20. Numerical analysis of LGU or LGF modules under various S#1 and S#2 walking conditions, with evidence of predicted vibration frequency variation: (a) DAM(top) or (b) DAM(LG2m) versus LGU models (ABAQUS).

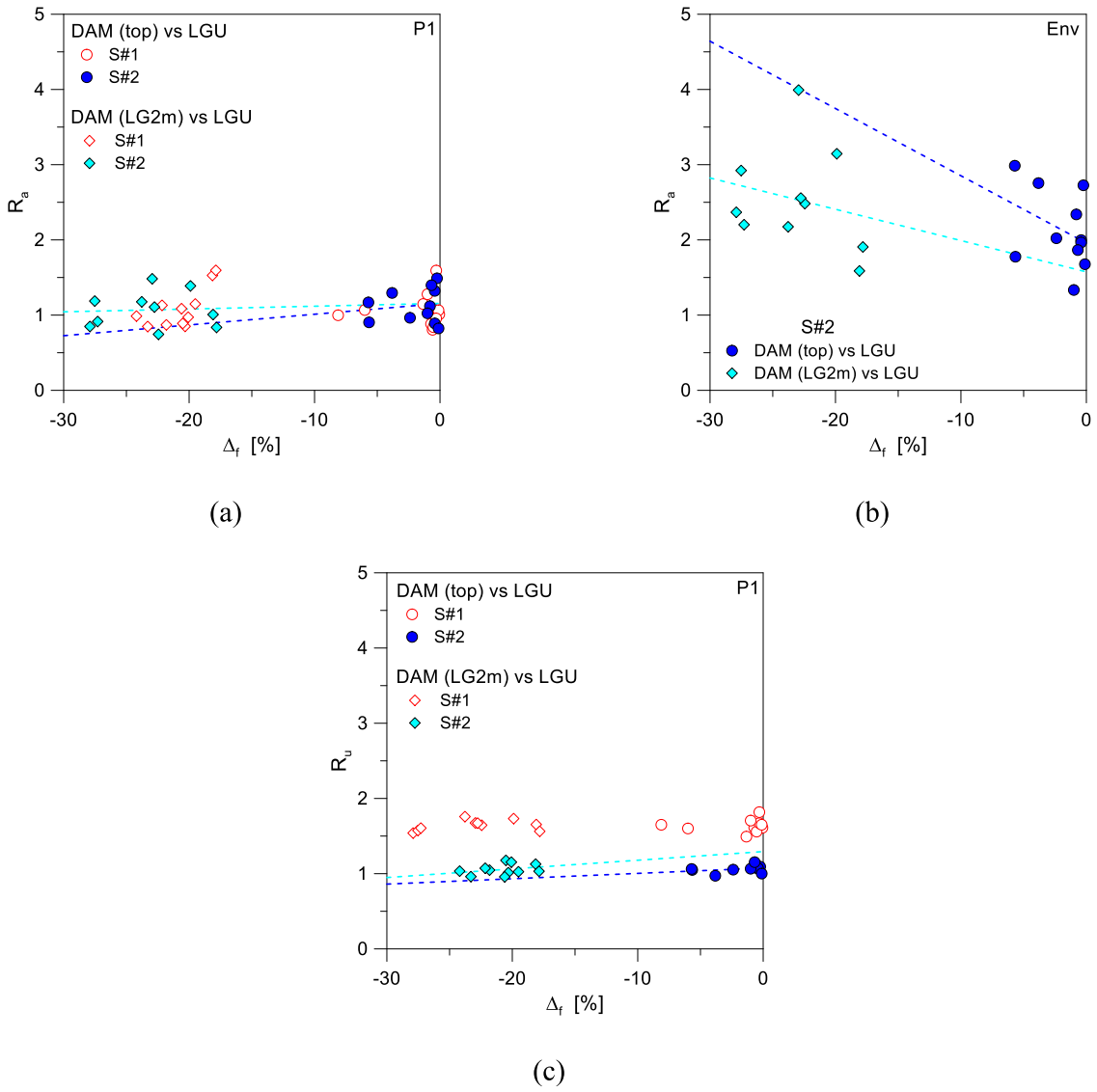

Fig. 21. Numerical analysis of LGU or LGF modules under various S#1 and S#2 walking conditions, with evidence of predicted (a)-(b) acceleration peak or (c) deflection ratio as a function of f_s (ABAQUS).

single mid-span node (i.e, P1 to P5 control points for the investigated modular units);

- In terms of absolute acceleration peaks on the structure, the use of conventional walking paths (like S#2 schemes in Fig. 17(a)) resulted in rather close correlation with experimental estimates of acceleration, both for uncracked (LGU) and damaged (LGF) slab modules;
- The use of conventional analytical walking paths (S#1 to S#3) in time-domain analysis for numerical signal processing and derivation of vibration frequencies for the occupied slab (i.e. Figs. 20 and 21), on the other side, was found not sufficiently accurate to derive appropriate mechanical considerations for structural monitoring assessment. In this regard, the use of conventional numerical procedures for damage investigations and quantitative predictions should be further addressed with the support of more extended experimental investigations;
- Finally, it is worth to note that the presently derived observations can be justified as far as the analysis is carried out on LG pedestrian components supported by knowledge in geometrical and mechanical properties (i.e., based on in-field experimental validation). Further uncertainty in the proposed procedure may derive from lack of calibration especially in terms of interlayer properties, which may result in marked viscoelastic behaviour and high sensitivity to operational conditions.

Data Availability Statement: Data will be available upon request.

Declaration of Competing Interest

The authors declare that they have no known competing financial interests or personal relationships that could have appeared to influence the work reported in this paper.

References

[1] CEN/TC 250. prCEN/TS xxxx-1: 2019—In-Plane Loaded Glass Components. CEN-European Committee for Standardization, Brussels, Belgium (2019).
[2] CEN/TC 250. prCEN/TS xxxx-2: 2019—Out of-Plane Loaded Glass Components. CEN-European Committee for Standardization, Brussels, Belgium (2019).
[3] CNR-DT 210/2013. Istruzioni per la progettazione, l'esecuzione ed il controllo di costruzioni con elementi strutturali di vetro. National Research Council of Italy (CNR): Roma, Italy, 2013 (in Italian).
[4] Bedon C, Zhang X, Santos F, Honfi D, Kozłowski M, Arrigoni M, et al. Performance of structural glass facades under extreme loads – Design methods, existing research, current issues and trends. Constr Build Mater 2018;163:921–37. https://doi.org/10.1016/j.conbuildmat.2017.12.153.

[5] Kott A, Vogel T. Controlling the post-breakage behavior of laminated safety glass. Proceedings of the International Symposium on the Application of Architectural Glass, Munich, 2004.
[6] Zhao C, Yang J, Wang X-e, Azim I. Experimental investigation into the post-breakage performance of pre-cracked laminated glass plates. Constr Build Mater 2019;224:996–1006.
[7] Galuppi L, Royer-Carfagni G. The post-breakage response of laminated heat-treated glass under in plane and out of plane loading. Compos B Eng 2018;147:227–39.
[8] Kozłowski M. Experimental and numerical assessment of structural behaviour of glass balustrade subjected to soft body impact. Compos Struct 2019;229:111380. https://doi.org/10.1016/j.compstruct.2019.111380.
[9] Bedon C, Kalamar R, Eliášová M. Low velocity impact performance investigation on square hollow glass columns via full-scale experiments and Finite Element analyses. Compos Struct 2017;182:311–25. https://doi.org/10.1016/j.compstruct.2017.09.055.
[10] Correia JR, Valarinho L, Branco FA. Post-cracking strength and ductility of glass-GFRP composite beams. Compos Struct 2011;93(9):2299–309.
[11] Corradi M, Speranzini E. Post-cracking capacity of glass beams reinforced with steel fibers. Materials 2019;12(2):231.
[12] Bedon C, Santarsiero M. Laminated glass beams with thick embedded connections – Numerical analysis of sull-scale specimens during cracking regime. Compos Struct 2018;195:308–24.
[13] Pelferne J, van Dam S, Kuntsche J, van Paepegem W. Numerical simulation of the EN 12600 Pendulum Test for Structural Glass. In Proceedings of the Challenging Glass Conference Proceedings, 16 June 2016; Volume 5, pp. 429–438, ISSN 2589-8019; 2016.
[14] Figuli L, Papan D, Papanova Z, Bedon C. Experimental mechanical analysis of traditional in-service glass windows subjected to dynamic tests and hard body impact. Smart Struct Syst 2021;27:365.
[15] Mohagheghian I, Wang Y, Zhou J, Yu L, Guo X, Yan Y, et al. Deformation and damage mechanisms of laminated glass windows subjected to high velocity soft impact. Int J Solids Struct 2017;109:46–62. https://doi.org/10.1016/j.ijsolstr.2017.01.006.
[16] Muralidhar S, Jagota A, Bennison SJ, Saigal S. Mechanical behaviour in tension of cracked glass bridged by an elastomeric ligament. Acta Mater 2000;48(18):4577–88.
[17] Seshadri M, Bennison SJ, Jagota A, Saigal S. Mechanical response of cracked laminated plates. Acta Mater 2002;50:4477–90.
[18] Delincé D, Callewaert D, Belis J, Van Impe R. Influence of temperature on post-breakage behaviour of laminated glass beams: Experimental approach. Proceedings of Challenging Glass 2 – Conference on Architectural and Structural Applications of Glass, TU Delft, May 2010, pp. 407-414.
[19] Pelfrene J, Kuntsche J, Van Dam S, Van Paepegem W, Schneider J. Critical assessment of the post-breakage performance of blast loaded laminated glazing: Experiments and simulations. Int J Impact Eng 2016;88:61–71.
[20] Zemanova A, Schmidt J, Sejnoha M. On pre- and post-fracture behaviour of laminated glass under bending. Int J Comp Meth and Exp Meas 2020;8(3):195–207.
[21] D'Ambrosio G, Galuppi L, Royer-Carfagni G. A simple model for the post-breakage response of laminated glass under in-plane loading. Compos Struct 2019;230:111426.
[22] Bedon C, Fasan M. Reliability of field experiments, analytical methods and pedestrian's perception scales for the vibration serviceability assessment of an in-service glass walkway. Appl Sci 2019;9(9).
[23] Bedon C. Diagnostic analysis and dynamic identification of a glass suspension footbridge via on-site vibration experiments and FE numerical modelling. Compos Struct 2019;216:366–78.
[24] Bedon C. Experimental investigation on vibration sensitivity of an indoor glass footbridge to walking conditions. J Build Eng 2020;29:101195.
[25] Bedon C, Noè S. Post-breakage vibration frequency analysis of in-service pedestrian laminated glass modular units. Vibration 4 (4), 836-852, https://doi.org/10.3390/vibration4040047.
[26] Zemanova A, Zeman J, Janda T, Schmidt J, Sejnoha M. On modal analysis of laminated glass: Usability of simplified methods and enhanced effective thickness. Compos B 2018;151:92–105.
[27] Lenci S, Consolini L, Clementi F. On the experimental determination of dynamical properties of laminated glass. Ann Solid Strut Mech 2015;7(1–2):27–43.
[28] Pelayo F, Lopez-Aenlle M. Natural frequencies and damping ratios of multi-layered laminated glass beams using a dynamic effective thickness. J Sandw Struct Mater 2017.
[29] Huang Z, Xie M, Du JZYM, Song H-K. Rapid evaluation of safety-state in hidden-frame supported glass curtain walls using remote vibration measurements. J Build Eng 2018;19:91–7.
[30] Gong M, Li Y, Shen R, Wei X. Glass suspension footbridge: human-induced vibration, serviceability evaluation, and vibration mitigation. J Bridge Eng November 2021;26(11). https://doi.org/10.1061/(ASCE)BE.1943-5592.0001788.
[31] Bedon C, Fasan M, Amadio C. Vibration analysis and dynamic characterization of structural glass element with different restraints based on operational modal analysis. Buildings 2019;9(1):13.
[32] Bedon C. Issues on the vibration analysis of in-service laminated glass structures: analytical, experimental and numerical investigations on delaminated beams. Appl Sci 2019;9(18):3928.
[33] ABAQUS Computer Software, Simulia, Dassault, RI, US, 2021.
[34] Sedlacek G, Heinemeyer C, Butz C. Generalisation of criteria for floor vibrations for industrial, office, residential and public building and gymnasium halls. Luxembourg: European Commission; 2006.
[35] Bachmann H, Ammann W. Vibrations in structures induced by man and machines. Can J Civ Eng 1987;15(6):1086–7.
[36] Al-Anbaki AF, Pavic A. Duality between time and frequency domains for vibration serviceability analysis of floor structures. Procedia Eng 2017;199:2759–65.
[37] Dimarogonas AD. Vibration of cracked structures: A state of the art review. Eng Fract Mech 1996;55(5):831–57.
[38] Salawu OS. Detection of structural damage through changes in frequency: a review. Eng Struct 1997;19(9):718–23.
[39] Shahabpoor E, Pavic A, Racic V. Interaction between walking humans and structures in vertical direction: A literature review. Shock Vib 2016;2016:3430285.
[40] Hearn G, Testa RB. Modal Analysis for Damage Detection in Structures. J Struct Eng October 1991;117(10).
[41] Limongelli MP, et al. Vibration Response-Based Damage Detection. In: Sause MGR, Jasiūnienė E, editors. Structural Health Monitoring Damage Detection Systems for Aerospace. Springer Aerospace Technology. Cham: Springer; 2021. https://doi.org/10.1007/978-3-030-72192-3_6.
[42] Hamey CS, Lastari W, Qiao P, Song G. Experimental damage identification of carbon/epoxy composite beams using curvature mode shapes. J Struct Health Monit 2004;3(4):333–53.
[43] Kim J-T, Ryu Y-S, Cho H-M, Stubbs N. Damage identification in beam-type structures: Frequency-based method vs mode-shape-based method. Eng Struct 2003;25(1):57–67.
[44] Liang H, Xie W, Wei P, Ai D, Zhang Z. Identification of dynamic parameters of pedestrian walking model based on a coupled pedestrian-structure system. Appl Sci 2021;11:6407. https://doi.org/10.3390/app11146407.
[45] Fangzhou L, Battini J-M, Pacoste C. Experimental and numerical analyses of single pedestrian walking on a hollow core concrete floor. Int J Civil Eng 2019;17:1201–9. https://doi.org/10.1007/s40999-018-0355-3.
[46] Figueiredo FP, da Silva JG, de Lima LR, de Andrade SA, Vellasco PD. A parametric study of composite footbridges under pedestrian walking loads. Eng Struct 2008;30(3):605–15.
[47] Cai Y, Gong G, Xia J, He J, Hao J. Simulations of human-induced floor vibrations considering walking overlap. SN Appl Sci 2020;2:19. https://doi.org/10.1007/s42452-019-1817-1.
[48] Han Z, Brownjohn JMW, Chen J. Structural modal testing using a human actuator. Eng Struct 2020;221(15):111113.
[49] Bedon C, Noè S. Uncoupled wi-fi body CoM acceleration for the analysis of lightweight glass slabs under random walks. J Sens Actuator Networks 2022;11(1):10. https://doi.org/10.3390/jsan11010010.
[50] Bedon C, Mattei S. Facial expression-based experimental analysis of human reactions and psychological comfort on glass structures in buildings. Buildings 2021;11:204. https://doi.org/10.3390/buildings11050204.
[51] SÉTRA (2996). Assessment of vibrational behavior of footbridges under pedestrian loading. In SÉTRA Technical Guide; Technical Department for Transport, Roads and Bridges Engineering and Road Safety: Paris, France.
[52] Clough RW, Penzien J. Dynamics of structures. Berkeley: McGrawHill; 1993.
[53] Bedon C, Bergamo E, Izzi M, Noè S. Prototyping and validation of MEMS accelerometers for structural health monitoring – The case study of the Pietratagliata cable-stayed bridge. J Sens Actuator Netw 2018;7:18.
[54] SMIT. Structural Modal Identification Toolsuite. 2021.
[55] Chang M, Leonard RL, Pakzad SN. SMIT User's Guide.
[56] Chang M, Pakzad SN. Observer Kalman filter identification for output-only systems using interactive structural modal identification toolsuite. J Bridge Eng 2014;19:04014002.